

Corrosion Fatigue Behavior of the High-Strength Magnesium Alloy AZ 80

M. Hilpert and L. Wagner

(Submitted 2 December 1999; in revised form 2 March 2000)

The fatigue performance of the high-strength magnesium alloy AZ 80 is studied in air as well as in aqueous 0.5 and 3.5% NaCl solutions. The effect of mechanical surface treatments, specifically mechanical polishing, shot peening, and roller burnishing on the S-N curves, is investigated using an electropolished surface as a reference. While mechanical polishing as well as shot peening improves fatigue performance in air, no improvement is observed in NaCl solutions. However, roller burnishing, which combines a smooth surface finish with residual compressive stresses in sufficient depths, leads to outstanding fatigue performance even in 3.5% NaCl solution.

Keywords fatigue, magnesium, alloy AZ 80, salt spray corrosion, surface treatment

1. Introduction

Owing to the potential reduction in weight for many structural parts, the application of magnesium alloys is expected to substantially increase in the next decade.[1] For automotive application, fatigue performance of magnesium alloys in aggressive environments is of particular importance. While mechanical surface treatments such as shot peening, roller burnishing, and deep rolling are known to improve the fatigue performance of structural metallic materials such as steels, aluminum, and titanium alloys,[2–5] there is little information on the influence of mechanical surface treatments on fatigue behavior of magnesium alloys. Furthermore, it is not known if mechanical surface treatments on magnesium alloys result in superior fatigue performance in aggressive environments. Thus, experimental data regarding suitable process parameters for mechanical surface treatments are needed. In the present investigation, the process parameters for shot peening as well as roller burnishing were varied widely to determine optimum conditions for fatigue life improvements of the high-strength magnesium alloy AZ 80.

2. Experimental

The high-strength magnesium alloy AZ 80 (nominal composition: 8.5Al, 0.5Zn, and 0.2Mn; balance: Mg) was received as extruded bar stock (100 mm diameter) from Otto Fuchs Metallwerke (Meinerzhagen, Germany). Specimens were machined with the load axis parallel to the extrusion (*L*) direction as well as parallel to the radial (*R*) direction, as illustrated in Fig. 1. Tensile and compressive tests were performed on threaded cylindrical specimens having gage lengths of 20 mm. Tensile properties as well as compressive yield stress of the as-received extrusion are given in Table 1.

The crystallographic texture of the bar stock was measured by neutron diffraction and was characterized by (0002) pole figures.

For fatigue testing, hour-glass-shaped cylindrical specimens (5 mm gage diameter) were machined. After machining, about 200 μm was removed from the surface of the specimens by electrolytical polishing to ensure that any machining effect that could mask the results was absent. This electrolytically polished condition **EP** is taken as the reference to which the various mechanical surface treatments will be compared. Mechanical polishing (**MP**) was done using an oil-bound paste with Al_20_3 particle sizes of 7 μm. Shot peening (**SP**) was performed with an injector type machine using either spherically conditioned cut wire SCCW14 (0.37 mm average shot size) or glass beads with average diameters of 0.66 mm. The Almen intensity was varied between 0.03 and 0.63 mm N. Roller burnishing (**RB**) was performed using a conventional lathe and a one-roll hydraulic system. The diameter of the hard-metal roll was 6 mm. The rolling forces were varied between 70 and 400 N.

Fatigue tests of the various conditions were performed under rotating beam loading ($R = -1$) at a frequency of about 60 Hz. Tests were done in ambient air as well as in aggressive environments using spray tests with aqueous 0.5 and 3.5% NaCl solutions. Fracture surfaces of the tensile and fatigue specimens were studied by scanning electron microscopy (SEM).

3. Results and Discussion

Most hcp magnesium grains in the as-received bar stock (location of texture measurement close to the center of the bar) are oriented with the basal planes parallel to the *L* direction and normal to the bar surface, while a much smaller volume fraction of grains is oriented with the basal planes perpendicular to the *L* direction (Fig. 2).

A microstructural texture in the bar stock is clearly seen by optical microscopy (Fig. 3), since second-phase stringers are present in the *L* direction as is typical for extrusions (Fig. 3a). The average α-grain size is roughly 30 μm (Fig. 3b).

M. Hilpert and **L. Wagner**, Chair of Physical Metallurgy and Materials Technology, Technical University of Brandenburg at Cottbus, 03013 Cottbus, Germany.

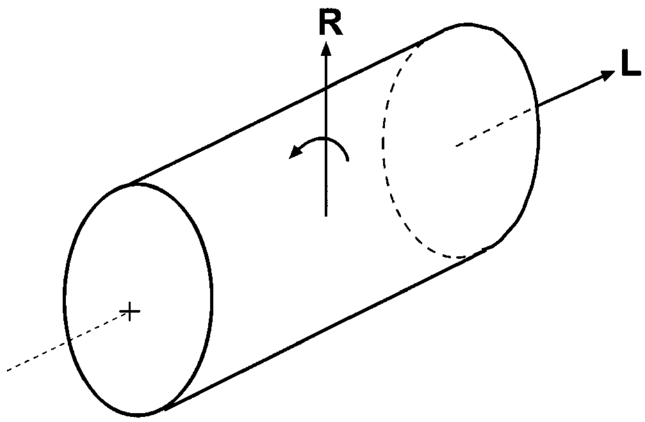

Fig. 1 As-received bar stock (*L*: longitudinal direction, *R*: radial direction)

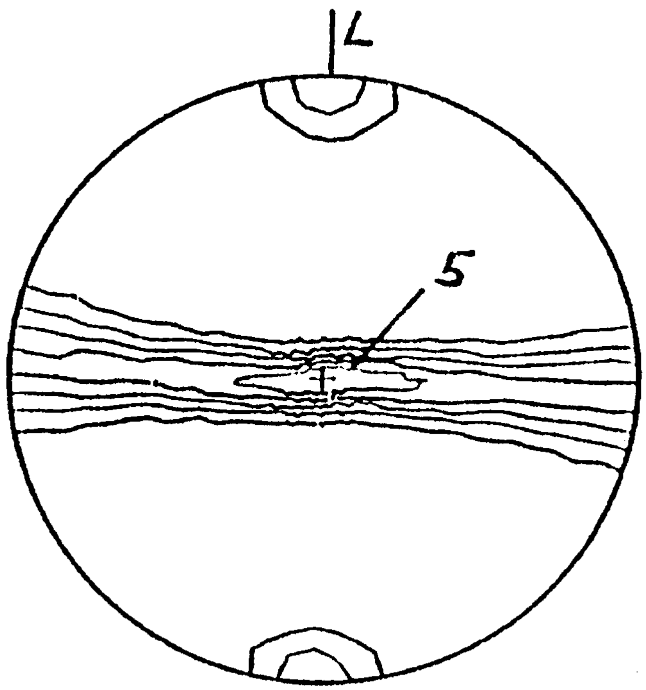

Fig. 2 (0002) pole figure of the as-received bar stock

Table 1 Tensile and compressive test results on AZ 80

Condition	Testing direction	$\sigma_{0.2T}$ (MPa)	$\sigma_{0.2C}$ (MPa)	UTS (MPa)	EL (%)	RA (%)
As received	*L*	225	185	350	9.3	12
	R	135	140	265	7.0	7

The tensile yield stress σ_{yT} in the *R* direction of the reference is only 60% of the corresponding value in the *L* direction (Table 1). Plastic deformation in the *R* direction is much easier than in the *L* direction, since basal planes experience large shear stresses by loading in the *R* direction, while hardly any shear stresses act on basal planes for loading in the *L* direction (Fig.

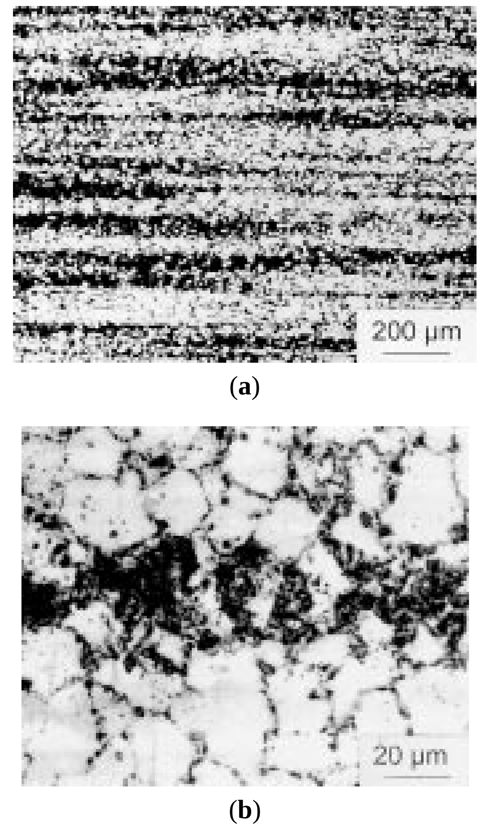

Fig. 3 (**a**) and (**b**) Microstructure of the as-received condition (*L*-axis horizontal)

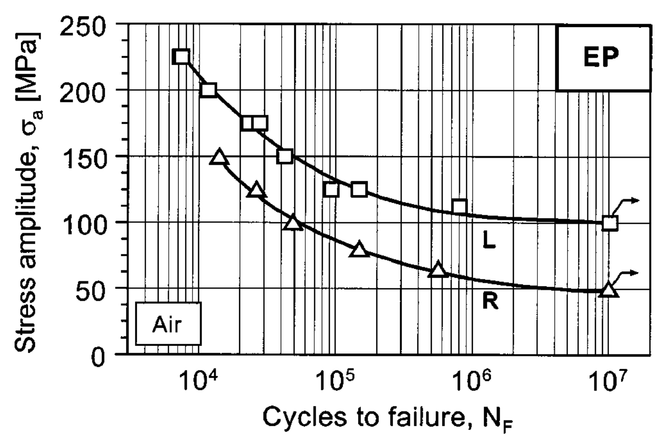

Fig. 4 S-N curves, $R = 1$, air, effect of loading direction (**EP**)

2). The compressive yield stress σ_{yC} is significantly lower than σ_{yT} in the L direction, while no marked difference in yield stress between tensile and compressive loading is found for the *R* direction (Table 1). This result can be explained by twinning on the pyramidal (1012) planes, since this type of twinning is favored when compressive stresses act parallel to the basal planes while it is impossible when stresses are perpendicular to the basal planes when $c/a < \sqrt{3}$ (6).

The S-N curves of the electropolished condition are shown in Fig. 4. The 10^7 cycles fatigue strength of **EP** for loading in

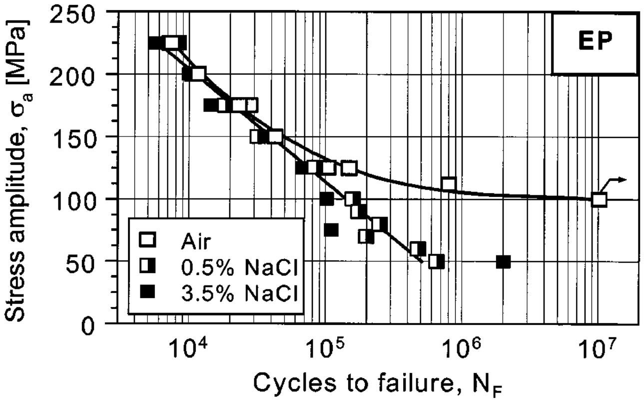

Fig. 5 S-N curves, $R = -1$, L direction, effect of environment (**EP**)

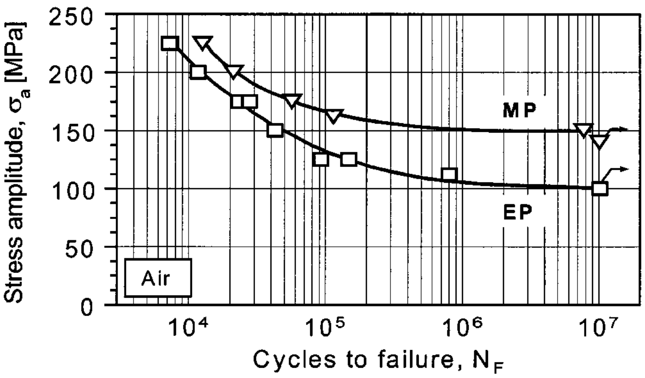

Fig. 6 S-N curves, $R = -1$, L direction, air, effect of polishing treatment

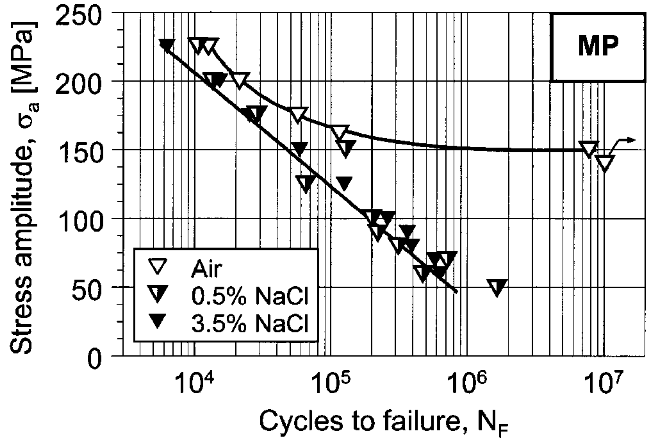

Fig. 7 S-N curves, $R = -1$, L direction, effect of environment (**MP**)

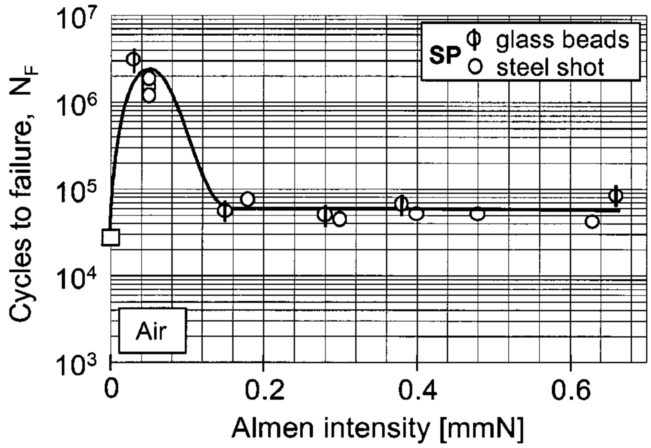

Fig. 8 Fatigue life (σ_a = 175 MPa) vs Almen intensity, effect of peening medium

the L direction is roughly twice that of the corresponding value in the R direction, indicating that the yield stress rather than tensile strength affects the fatigue strength.[7] The effect of environment on the fatigue results for loading in the L direction is illustrated in Fig. 5. Above stress amplitudes of 125 MPa, the aggressive environment does not lead to a significant reduction in life time in air irrespective of the NaCl concentration. While the fatigue life in air is clearly reduced at stress amplitudes lower than 125 MPa, there is again no difference in fatigue life between testing in 0.5 or 3.5% NaCl solution. From the strong stress amplitude dependence of the environmental effect, it is derived that in magnesium alloys, fatigue crack nucleation rather than propagation is predominantly affected by the aggressive environment.

Mechanical polishing as opposed to **EP** results in a significant fatigue life improvement in AZ 80, particularly in the HCF region (Fig. 6). Similar results were reported on titanium alloys and are explained by process-induced high dislocation densities in near-surface regions, improving the materials resistance to nucleating fatigue cracks.[8] Note that **MP** can increase the 10^7 cycles fatigue strength of the virgin material **EP** by as much as 50% (Fig. 6). Unlike the fatigue results of the reference, after mechanical polishing, there is a marked reduction in fatigue life owing to the aggressive environment (0.5 or 3.5% NaCl solutions) already at stress amplitudes higher than 125 MPa (Fig. 7). Comparing Fig. 7 with Fig. 5, it can be seen that the fatigue life of **EP** and **MP** is very similar in aggressive environments. Obviously, a high dislocation density in a very thin layer as present after **MP** is not able to increase the resistance to fatigue crack nucleation in aggressive environments.

The effect of peening medium and Almen intensity on fatigue life after **SP** is shown in Fig. 8. Starting with the electropolished condition, the fatigue life first dramatically increases by roughly two orders of magnitude irrespective of the particular peening medium and then drops drastically after peening with higher intensities. This strong overpeening effect was also found at stress amplitudes of σ_a = 225 and 200 MPa.[9] As seen in Fig. 9, subsurface fatigue crack nucleation was found under optimum peening conditions (Fig. 9b), while fatigue cracks nucleated at the surface not only in the reference (Fig. 9a) but also after peening with higher Almen intensities (Fig. 9c). Note that when fatigue cracks nucleate subsurface, crack nucleation as well as early crack propagation occurs under vacuum conditions.[10]

Again, this shift in crack nucleation site was independent of the particular peening medium used. Similar results were reported in earlier work on titanium alloys.[10] With an increase in Almen intensity, a significantly higher number of fatigue

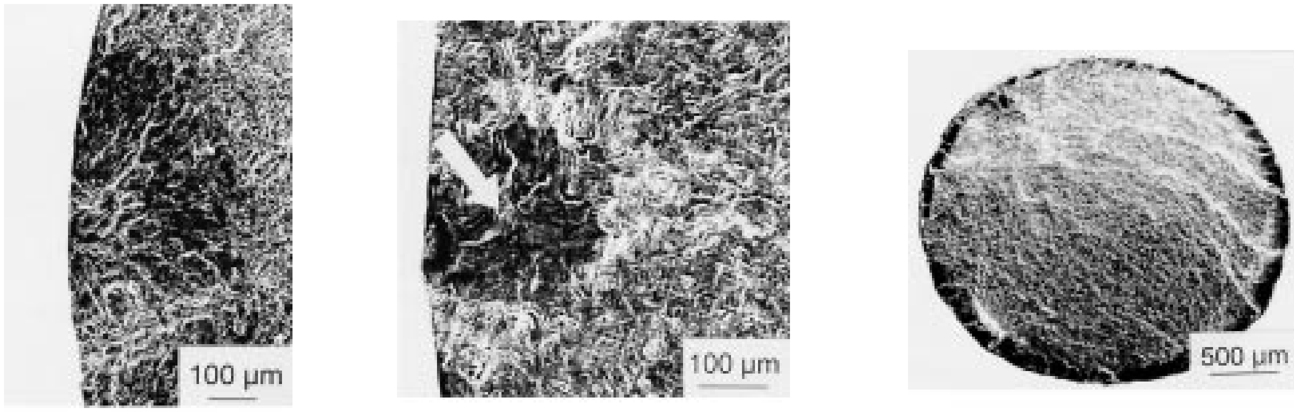

a) at surface (EP) b) subsurface (SP, 0.05 mmN) c) at surface (SP, 0.40 mmN)

Fig. 9 (**a**), (**b**), and (**c**) Fatigue crack nucleation sites (SEM)

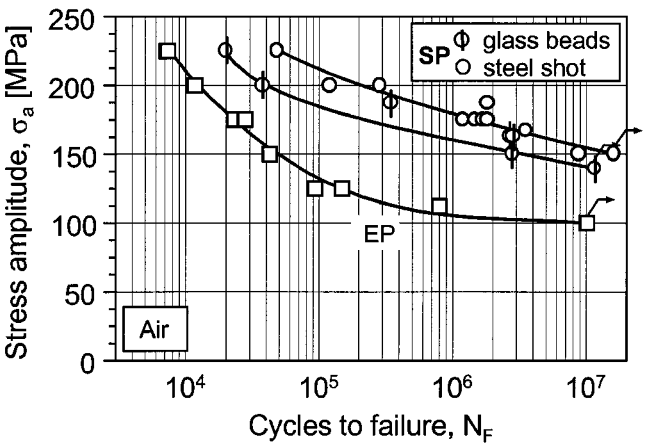

Fig. 10 S-N curves, $R = -1$, L direction, air, effect of peening treatment

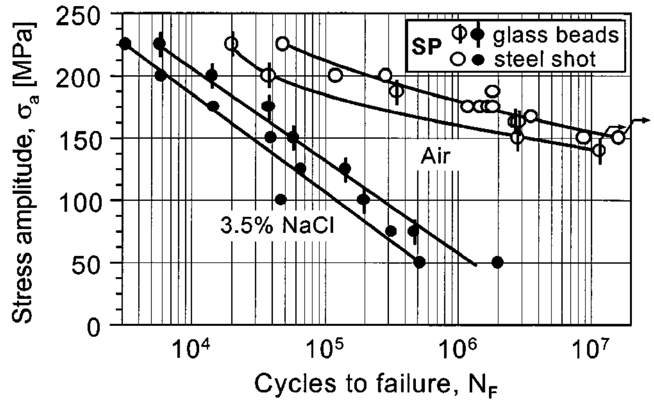

Fig. 11 S-N curves, $R = -1$, L direction, effect of environment (**SP**)

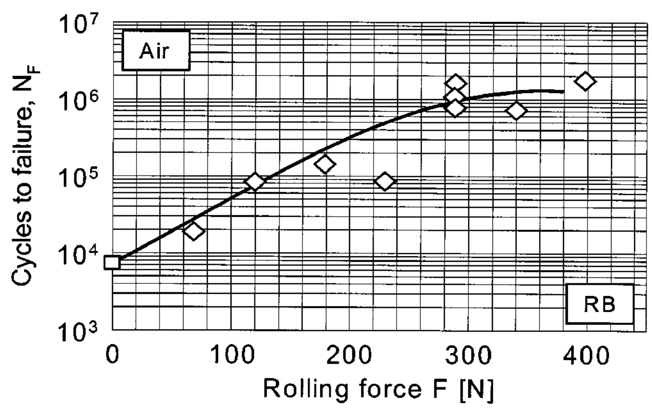

Fig. 12 Fatigue life (σ_a = 225 MPa) vs rolling force (**RB**)

crack nucleation sites at the surface was found. In addition, numerous secondary cracks, which did not propagate, were seen, particularly on specimens shot peened to higher intensities, indicating a pronounced effect of surface roughness on the resistance to fatigue crack nucleation.

The effect of optimum **SP** treatments on the S–N curves in air is illustrated in Fig. 10. Compared to the reference **EP**, there is a very marked improvement in fatigue life at all stress amplitudes due to **SP**. On average, the fatigue performance of specimens peened with steel shot is slightly superior to those peened with glass beads. Comparing the fatigue results on shot peened specimens between air and NaCl solutions (Fig. 11), it is evident that the aggressive environment markedly reduces fatigue life. Since the ranking of the peening media with regard to fatigue performance changes between tests in air and in a NaCl solution (Fig. 11), the loss in fatigue life is particularly pronounced for specimens peened with steel shot. Presumably, iron contamination of the magnesium surface leads to an additional adverse effect of the NaCl environment.[11]

The effect of the rolling force on the fatigue life for **RB** is shown in Fig. 12. Starting with the reference, the fatigue life strongly increases with rolling force. Highest improvements in lifetime of roughly two orders of magnitude are realized, by rolling with forces equal or greater than 285 N. Similar to the results after optimum **SP** treatments, fatigue cracks nucleate subsurface (Fig. 13), however, at distances from the surface much greater than after **SP** (compare Fig. 13 with 9b).

The effect of optimum **RB** on the S–N curves in air is

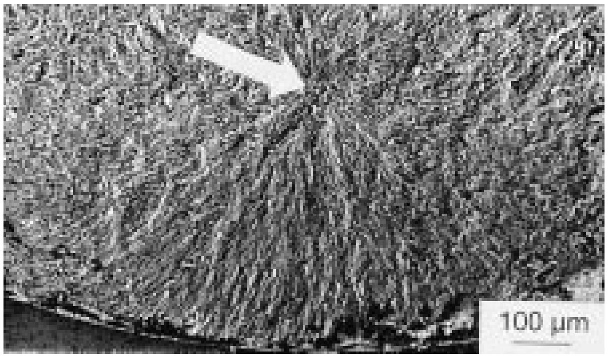

Fig. 13 Subsurface fatigue crack nucleation (SEM), $F = 285$ N (**RB**)

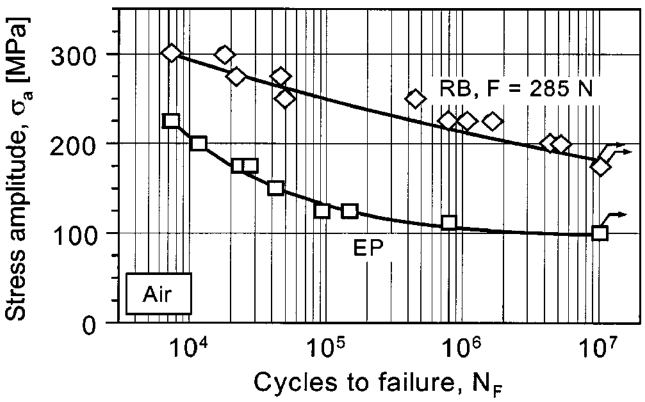

Fig. 14 S-N curves, $R = -1$, L direction, air, effect of **RB**

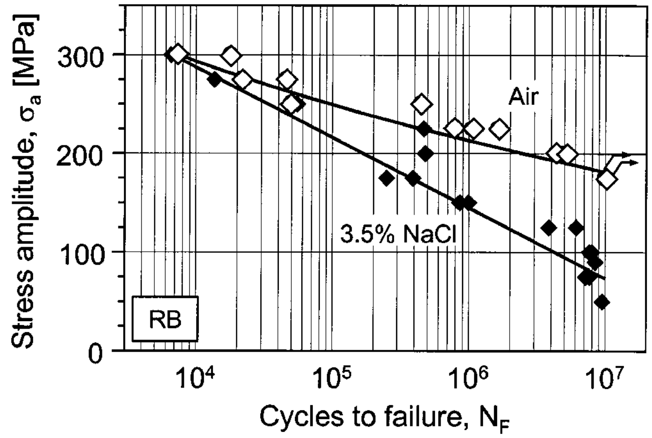

Fig. 15 S-N curves, $R = -1$, L direction, effect of environment (**RB**)

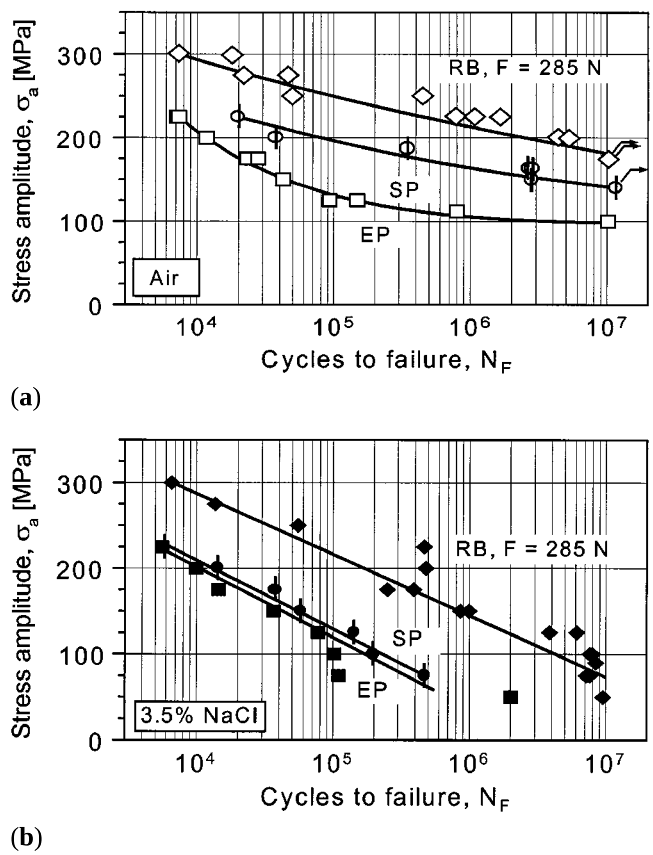

Fig. 16 S-N curves, $R = -1$, L direction, effect of surface treatment: (**a**) air and (**b**) 3.5 NaCl solution

illustrated in Fig. 14. The improvement of the fatigue performance due to optimum **RB** is even higher than after optimum **SP** (compare Fig. 14 with 12). From parallel work, it is known that the surface roughness after **RB** even for the highest rolling forces is as low as in the reference, while **SP** at least at higher intensities drastically roughens the surface. Shot peening at higher intensities, which may result in plastically deformed depths comparable to those after **RB**, can lead to marked lifetime improvements only if an additional surface smoothening, *e.g.*, by **MP** is applied.[7] The effect of the aggressive NaCl solution as opposed to air on the fatigue performance of the **RB** condition is shown in Fig. 15. Below stress amplitudes of 200 MPa, the fatigue life in 3.5% NaCl solution is significantly lower than in air.

For comparison, the fatigue results of the conditions **RB** and **SP** are replotted in Fig. 16. For tests in air (Fig. 16a), peening with glass beads already results in substantial improvements in fatigue life of the reference, while RB by far gives the best results. For tests in 3.5% NaCl solution, peening with glass beads hardly improves the fatigue performance of the reference. On the contrary, **RB** increases the fatigue life in 3.5% NaCl solution by at least one order of magnitude. The shape of the S–N curves in 3.5% NaCl solution (Fig. 16b), which is typical for crack propagation dominated fatigue life and is in contrast to the knee geometry of the S–N curves in air (Fig. 16a), indicates that fatigue cracks nucleate early in all three conditions. Since peening results in almost no fatigue life improvement, although process-induced residual compressive stresses clearly retard microcrack growth,[9] fatigue cracks after peening must nucleate much earlier than in the reference **EP**. Finally, the outstanding performance of AZ 80 after **RB** is the result of both the smooth surface and residual compressive stresses in sufficient depths.

Acknowledgments

The authors thank Otto Fuchs Metallwerke (Meinerzhagen, Germany) for providing the magnesium alloy. Thanks are also due to Dr. Brokmeier, Technical University Clausthal (Clausthal, Germany), for performing the texture measurements by neutron diffraction.

References

1. T.K. Aune and H. Westengen: in *Magnesium Alloys and Their Applications*, B.L. Mordike and F. Hehmann, eds., DGM, Oberursel, Germany, 1992, p. 221.
2. C.H. Burck, C.P. Sullivan, and C.H. Wells: *Metall. Trans.*, 1970, vol. 1, p. 1995.
3. M.S. Baxa, Y.A. Chang, and C.H. Burck: *Metall. Trans. A*, 1979, vol. 9A, p. 656.
4. J.E. Hack and G.R. Leverant: *Residual Stress Effects in Fatigue*, ASTM STP 776, ASTM, Philadelphia, PA, 1982, p. 204.
5. H. Gray, L. Wagner, and G. Lütjering: *Residual Stresses in Science and Technology*, DGM, Oberursel, Germany, 1987, p. 815.
6. M. Hilpert, A. Styczynski, J. Kiese, and L. Wagner: in *Magnesium Alloys and Their Applications*, B.L. Mordike and K.U. Kainer, eds., MAT INFO, Frankfurt, Germany, 1998, p. 319.
7. M. Hilpert and L. Wagner: in *Magnesium Alloys and Their Applications*, B.L. Mordike and K.U. Kainer, eds., Mat Info, Frankfurt, Germany, 1998, p. 271.
8. L. Wagner: *ASM Handbook*, vol. 19, *Fatigue and Fracture*, ASM International, Materials Park, OH, 1996, p. 839.
9. M. Hilpert and L. Wagner: in *Automotive Alloys III*, S.K. Das, ed., TMS, Warrendale, PA, 1999.
10. L. Wagner and G. Lütjering: in *Shot Peening*, H.O. Fuchs, ed., American Shot Peening Society, Paramus, NJ, 1984, p. 194.
11. D. Deiseroth, W. Zinn, and B. Scholtes: in *Magnesium Alloys and Their Applications*, B.L. Mordike and K.U. Kainer, eds., Mat Info, Frankfurt, Germany, 1998, p. 409.